

# Structure and morphology of self-assembled 3-mercaptopropyltrimethoxysilane layers on silicon oxide

Minghui Hu<sup>\*</sup>, Suguru Noda, Tatsuya Okubo, Yukio Yamaguchi, Hiroshi Komiyama

Department of Chemical System Engineering, The University of Tokyo

7-3-1 Hongo, Bunkyo-ku, Tokyo 113-8656 JAPAN

phone: +81-3-5841-7330, fax: +81-3-5841-7230, e-mail: mhu@chemsys.t.u-tokyo.ac.jp

## Abstract

Self-assembled 3-mercaptopropyltrimethoxysilane (MPTMS,  $(\text{CH}_3\text{O})_3\text{SiCH}_2\text{CH}_2\text{CH}_2\text{SH}$ ) layers on hydroxyl-terminated silicon oxide ( $\text{SiO}_2$ ) were prepared at MPTMS concentrations ranging from  $5 \times 10^{-3}$  M to  $4 \times 10^{-2}$  M. The surface structure and morphology of MPTMS layers were characterized by X-ray photoelectron spectroscopy (XPS), contact angle measurements, scanning electron microscopy (SEM), and atomic force microscopy (AFM). We found that the MPTMS layers on  $\text{SiO}_2$  consisted of dispersed domains 20-200 nm in diameter, instead of continuous, flat monolayers. With increasing MPTMS concentration, the domain shape changed from flat to steep. Flat domains were composed of well-ordered monolayers with thiol headgroups uniformly distributed on the uppermost surface, whereas steep domains were composed of disordered polymers with randomly distributed thiol headgroups on the uppermost surface. These results indicate that MPTMS molecules show good self-assembly at an MPTMS concentration of  $5 \times 10^{-3}$  M, but not above this concentration. The effect of MPTMS concentration on the structure and morphology of MPTMS layers might be due to the competition between self-polymerization and surface dehydration reactions, which depends on the trace quantity of water in the solvent and on

the SiO<sub>2</sub> surface. Our research further indicates that MPTMS and water concentrations are the controlling parameters for preparing well-ordered, self-assembled MPTMS monolayers on SiO<sub>2</sub>.

**PACS:** 68.35.Bs; 82.65.My; 81.65.Ya

**Keywords:** Surface modification; Silicon oxide; Self-assembled monolayers; Atomic force microscopy; X-ray photoelectron spectroscopy

## 1. Introduction

Long-chain alkyltrichlorosilanes and alkyltrimethoxysilanes, such as octadecyltrichlorosilane (OTS, C<sub>18</sub>H<sub>37</sub>SiCl<sub>3</sub>), are known to form closely packed, well-ordered, self-assembled monolayers (SAMs) on hydroxyl-terminated SiO<sub>2</sub> surfaces. In the 1990's, these compounds received much attention in the field of materials science because they offer unique opportunities for increasing the fundamental understanding of self-organization, structure-property relationships, and interfacial phenomena [1]. Recently, the characteristics of these SAMs, i.e., chemical composition, chain orientation, film thickness, and surface coverage characteristics, have been extensively investigated by using X-ray photoelectron spectroscopy (XPS), atomic force microscopy (AFM), scanning tunneling microscopy (STM), ellipsometry, Fourier transform infrared spectroscopy (FT-IR), and contact angle measurements [2-7]. Parameters, such as concentration, solvent properties, temperature, and reaction time play important roles in SAMs formation [2-4]. Furthermore, it was found that some SAMs have disordered heterogeneous domain structures [5-7].

Most of the previous research on SAMs, however, has mainly been focused on SAMs without terminal functional groups. Very little research has been done on SAMs with terminal functional groups, such as H<sub>2</sub>N-, HO-, HS-, HSO<sub>3</sub>-, Cl-, and Br-, because the introduction of a polar terminal functional group causes the formation of more disordered monolayers [8-11]. Even in such research,

the surface structure and morphology of SAMs were studied independently, and their relation has rarely been described. Understanding the structure and morphology of SAMs with terminal functional groups is important because these SAMs are useful in scientific and technological fields, such as analytical chemistry [12], biochemistry [13], crystallography [14], electronics [15], and optics [16].

In this work, we studied the surface structure and morphology of self-assembled 3-mercaptopropyltrimethoxysilane (MPTMS,  $(\text{CH}_3\text{O})_3\text{SiCH}_2\text{CH}_2\text{CH}_2\text{SH}$ ) layers on hydroxyl-terminated  $\text{SiO}_2$  surfaces formed by MPTMS at various MPTMS concentrations in benzene. We selected MPTMS because it is terminated with thiol. Organosulfur compounds, such as alkanethiol and dialkyl disulfide etc., have a strong affinity for transition metal surfaces, which form SAMs on metals [17-20] and semiconductors [21-23]. The MPTMS layers with a thiol-terminated uppermost surface can serve as an important coupling agent between transition metals and silicon oxides [24-26]. Therefore, they are promising for controlling wetting, corrosion inhibition, protein adsorption, catalysis, electronics, and biosensors. In this paper, therefore, we discuss the effect of MPTMS concentration on the surface structure and morphology of MPTMS layers formed on  $\text{SiO}_2$ , and suggest that to prepare well-ordered, self-assembled MPTMS monolayers, it is important to precisely control the MPTMS and water concentrations in solvents.

## 2. Experimental

### 2.1. Materials

P-type, <100> oriented silicon wafers were provided by Shin-Etsu Chemical Co., Ltd. and MPTMS (purity: 85%) was purchased from Aldrich Chemicals. Hydrofluoric acid (HF), hydrogen peroxide ( $\text{H}_2\text{O}_2$ ), and concentrated sulfuric acid ( $\text{H}_2\text{SO}_4$ ) were purchased from Wako Pure Chemicals Industries, Ltd. and used for substrate treatment. Water was deionized by using a

Millipore-W system equipped with cation and anion exchange columns. Anhydrous grade benzene, chloroform, and methanol were purchased from Wako Pure Chemicals Industries, Ltd. and used as received. The quantity of H<sub>2</sub>O in all the solvents was less than 30 ppm.

## 2.2. Substrate preparation

Silicon wafers were cut into 1×1 cm pieces, sonicated in ethanol for 10 min, and rinsed with deionized (DI) water. To remove the natural oxide layer, the substrates were dipped into a 1% HF solution for 3 minutes, followed by rinsing with DI water. Finally, 5-10 nm thick SiO<sub>2</sub> films were deposited on these substrates by using radio frequency (RF) magnetron sputtering. These substrates with sputtered SiO<sub>2</sub> thin films were used as the substrates for the formation of self-assembled MPTMS layers.

## 2.3. Formation of self-assembled MPTMS layers

First, we hydroxylated SiO<sub>2</sub> surfaces by soaking the substrates in 1N HNO<sub>3</sub> for 24 hours. Then, the substrates were rinsed and further hydroxylated by immersing them in a 30:70 (v/v) mixture of H<sub>2</sub>O<sub>2</sub> and H<sub>2</sub>SO<sub>4</sub> at 60-80 °C for 30 min. The resulting SiO<sub>2</sub> surface was considered to have about 5 OH groups per nm<sup>2</sup> [27, 28]. The substrates were dried under an nitrogen (N<sub>2</sub>) stream and further dried by heating in an oven at 100 °C for 30 min.

MPTMS solutions at concentrations ranging from 5×10<sup>-3</sup> M to 4×10<sup>-2</sup> M in benzene were prepared in an N<sub>2</sub> atmosphere. The substrates with SiO<sub>2</sub> thin films were immersed into MPTMS solutions at room temperature for 30 minutes in an N<sub>2</sub> atmosphere. The substrates were taken out and then successively washed with benzene, chloroform, methanol, DI water, and finally dried in an N<sub>2</sub> stream. For comparison, samples were also prepared with the same treatment procedure, but without adding MPTMS. We refer to these samples as bare SiO<sub>2</sub> in this paper.

## 2.4. Analysis

X-ray photoelectron spectroscopy (XPS) and angle-resolved X-ray photoelectron spectroscopy (ARXPS) were measured with a RIGAKU XPS-7000 spectrometer using an Mg K $\alpha$  (1253.6 eV) source at a power level of 200 W. Each sample was analyzed at a photoelectron take-off angle of 90°, except for the angle-resolved measurements, which were analyzed with take-off angles ranging from 10° to 90°. The take-off angle is defined as the angle between the analyzer and the substrate surface. The binding energy (BE) scale was calibrated to 284.8 eV (-CH<sub>2</sub>-CH<sub>2</sub>-SiO<sub>3</sub><sup>3-</sup>) for the main C(1s) (C-C, C-H and C-Si) feature [29].

The water contact angle on SiO<sub>2</sub> treated with MPTMS was measured at room temperature at three different positions on each sample by using a contact angle analyzer (KYOWA, FACE CA-DT·A).

The surface morphology was characterized with SEM and AFM measurements. SEM measurements were made with a field emission scanning electron microscope (FE-SEM) (HITACHI S-900). Before loading into the observation chamber, we coated all of the samples with Pt by ion sputtering to compensate for the charging effect of sample surfaces. AFM measurements were made with a Nanoscope IIIa (Digital Instruments) equipped with a MultiMode microscope operated in the tapping mode, in air, and at room temperature.

## 3. Results and discussion

### 3.1. Structure of self-assembled MPTMS layers

The relative elemental compositions of MPTMS-treated SiO<sub>2</sub> surfaces measured with XPS are listed in Table 1. The elemental fraction of sulfur and carbon on SiO<sub>2</sub> surfaces increased after the

treatment with MPTMS, which indicates that MPTMS was introduced to SiO<sub>2</sub> surfaces. As the MPTMS concentration increased from  $5 \times 10^{-3}$  M to  $4 \times 10^{-2}$  M, the C/S atomic ratio, which was expected to be 3:1 from the MPTMS molecular composition, decreased from 20:1 to 6:1. This excess carbon above the expected ratio of 3:1 might be due to contamination of organic chemicals, such as solvents or impurities in the air.

Figure 1 shows high-resolution XPS spectra of C(1s) for SiO<sub>2</sub> substrates before and after treatment with  $5.0 \times 10^{-3}$  M and  $4.0 \times 10^{-2}$  M MPTMS, which indicate the existence of MPTMS on SiO<sub>2</sub> surfaces. The C(1s) XPS spectrum of bare SiO<sub>2</sub> substrate shows only one band at 284.8 eV, whereas those of the SiO<sub>2</sub> substrates treated with  $5.0 \times 10^{-3}$  M and  $4.0 \times 10^{-2}$  M MPTMS show two contribution bands, centered at 284.8 and 286.4 eV, respectively. The band at 284.8 eV corresponds to hydrocarbon and carbon bonded to silicon (C-C, C-H, and C-Si, 284.8 eV peak), and the band at 286.4 eV corresponds to carbon bonded to oxygen and sulfur (C-O and C-S, 286.4 eV peak) [16]. The appearance of a new band of C(1s) at 286.4 eV demonstrates the reaction of MPTMS with SiO<sub>2</sub> surfaces after the treatment with MPTMS. Furthermore, for all the samples, the dominant component (C-C, C-H, and C-Si) occupied about 75% of the overall carbon, which is larger than the 66% expected from the MPTMS molecular composition. We attribute this excess hydrocarbon to contamination, which agrees with the previous discussion about the C/S atomic ratio on SiO<sub>2</sub> after the treatment with MPTMS.

We investigated the chemical state of sulfur in MPTMS layers on SiO<sub>2</sub> by using ARXPS. High-resolution XPS spectra of S(2p) for SiO<sub>2</sub> substrates treated with  $5.0 \times 10^{-3}$  M and  $4.0 \times 10^{-2}$  M MPTMS are shown in Fig. 2. The ARXPS profiles were obtained at take-off angles varying from 10° to 90°. All the data can be fitted with a single Gaussian curve, which indicates that sulfur only exists in a single chemical state in MPTMS layers formed by both  $5.0 \times 10^{-3}$  M and  $4.0 \times 10^{-2}$  M MPTMS. In other words, the interaction between thiols and surface silanols is negligible. For SAMs on SiO<sub>2</sub> formed by amine-functionalized 3-aminopropyltrimethoxysilane (APTES, (CH<sub>3</sub>CH<sub>2</sub>O)<sub>3</sub>SiCH<sub>2</sub>CH<sub>2</sub>CH<sub>2</sub>NH<sub>2</sub>), however, different results have been reported [8-11]. The N(1s)

XPS signal shows two components assigned to free amine, and to hydrogen-bonded and protonated amine, respectively. Kallury et al. reported that either surface water or surface silanols promote the amine-surface interaction and orient the amino moieties towards the SiO<sub>2</sub> surface [9]. The strong interaction between functional groups and surface silanols interferes with the formation of well-oriented SAMs. Therefore, self-assembled MPTMS layers appear to have better orientation than APTES layers on SiO<sub>2</sub>, owing to the weaker interaction between thiols and surface silanols than between amines and surface silanols.

To evaluate the orientation of MPTMS molecules in MPTMS layers on SiO<sub>2</sub>, the variation of S/C atomic ratio was derived from ARXPS analysis, which is shown in Fig. 3. As the take-off angle decreased, the S/C atomic ratio increased for samples treated with  $5.0 \times 10^{-3}$  M MPTMS, but was almost constant for samples treated with  $4.0 \times 10^{-2}$  M MPTMS. This demonstrates that at the MPTMS concentration of  $5.0 \times 10^{-3}$  M, MPTMS forms well-ordered layers with thiol headgroups uniformly distributed on the uppermost surface. At the MPTMS concentration of  $4.0 \times 10^{-2}$  M, however, MPTMS forms disordered layers with randomly distributed thiol headgroups, i.e., MPTMS polymers, as discussed later.

Figure 4 shows the variation of water contact angle on SiO<sub>2</sub> treated with MPTMS at MPTMS concentrations ranging from 0 to  $8.0 \times 10^{-2}$  M. The contact angle for bare SiO<sub>2</sub> was 46°. For other samples treated with MPTMS, at MPTMS concentrations ranging from  $5.0 \times 10^{-3}$  M to  $8.0 \times 10^{-2}$  M, the contact angle increased from 71° to 104°. Heise et al. reported that the contact angles of SAMs formed by using methyl- and amine-terminated alkylsiloxanes on SiO<sub>2</sub> were 68° and 103°, respectively [30]. We consider that our measured contact angle of 71° is due to well-ordered structures with thiol headgroups distributed on the uppermost surface, whereas our measured contact angle of 104° is due to disordered structures with randomly orientated thiol groups distributed on the uppermost surface. This is consistent with our investigations made with ARXPS. Therefore, both ARXPS and contact angle measurements demonstrate that using MPTMS at the low concentration of  $5.0 \times 10^{-3}$  M is effective for forming well-ordered layers with thiol headgroups on

the uppermost surface. At higher MPTMS concentrations than this, however, MPTMS molecules lose the self-assembly.

### 3.2. Morphology of self-assembled MPTMS layers

The surface morphology of assembled MPTMS layers formed on SiO<sub>2</sub> substrates was investigated with FE-SEM and AFM. Figure 5 shows FE-SEM images of bare SiO<sub>2</sub> surface (Fig. 5a) and SiO<sub>2</sub> surfaces treated with MPTMS at MPTMS concentrations of  $5 \times 10^{-3}$  M,  $2 \times 10^{-2}$  M, and  $4 \times 10^{-2}$  M (Fig. 5b, 5c and 5d), respectively. In comparison with the smooth, bare SiO<sub>2</sub> surface (Fig. 5a), the surface roughness increased with increasing MPTMS concentration, which can be seen from the increase of image contrast in Figs. 5b to 5d. For samples treated with  $5.0 \times 10^{-3}$  M MPTMS (Fig. 5b), only a few, small irregularities with sizes below several tens of nanometers were observable. For samples treated with  $4.0 \times 10^{-2}$  M MPTMS (Fig. 5d), however, many large irregularities appeared, with sizes ranging from several tens to several hundreds of nanometers. It is conceivable that such irregularities are MPTMS polymers rather than MPTMS monolayers. These results support the fact that the increase of MPTMS polymers on SiO<sub>2</sub> surfaces leads to an increase of disordered orientation of MPTMS layers.

SEM images only provide two-dimensional information about MPTMS layers, but for proper analysis of sizes and shape of irregularities, three-dimensional information of such irregularities is needed. Therefore, as shown in Fig. 6, we used AFM to determine three-dimensional surface morphologies. The top panels show AFM images of surfaces of bare SiO<sub>2</sub> (Fig. 6a), and SiO<sub>2</sub> after the treatment with MPTMS (Fig. 6b, 6c and 6d). The bottom panels show contours of cross-sections along the diagonal from the top left to the bottom right of each image shown in the corresponding top panel. In contrast to the smooth surface of bare SiO<sub>2</sub>, MPTMS layers formed at MPTMS concentrations ranging from  $5.0 \times 10^{-3}$  M to  $4.0 \times 10^{-2}$  M consisted of dispersed domains, with sizes ranging from 20 to 200 nm in diameter, and shape varying from flat for samples treated with

$5.0 \times 10^{-3}$  M MPTMS (Fig. 6b), to steep for samples treated with  $4.0 \times 10^{-2}$  M MPTMS (Fig. 6d).

The height of these domains can be seen from the contours of the MPTMS layer cross-sections along the diagonal, as shown in the bottom panels in Fig. 6. For samples treated with  $5.0 \times 10^{-3}$  M (Fig. 6b), there were many domains less than 1 nm high, and a few domains 2-3 nm high. Samples treated with  $2.0 \times 10^{-2}$  M MPTMS (Fig. 6c) had domains that were typically 2-3 nm high, while those treated with  $4.0 \times 10^{-2}$  M MPTMS (Fig. 6d) had domains mostly higher than 5 nm. The domains less than 1 nm high are self-assembled MPTMS monolayers because the thickness of one monolayer of MPTMS is about 0.7 nm [8, 26], whereas the domains 2-3 nm high or larger are disordered MPTMS polymers. For samples treated with  $5.0 \times 10^{-3}$  M MPTMS (Fig. 6b), although the SiO<sub>2</sub> surface was covered with a mixture of monolayers and polymers, the percentage of monolayers was much larger than polymers. For samples treated with  $4.0 \times 10^{-2}$  M MPTMS (Fig. 6d), however, most domains were much higher than one monolayer thickness of MPTMS, and were therefore considered as MPTMS polymers. Although a few domains with thickness close to MPTMS monolayers can be seen, the SiO<sub>2</sub> surface was almost completely covered with MPTMS polymers.

The effect of MPTMS concentration on the structure and morphology of MPTMS layers on SiO<sub>2</sub> substrates is summarized in Fig. 7. For MPTMS concentrations ranging from  $5 \times 10^{-3}$  M to  $4 \times 10^{-2}$  M, the MPTMS layers on SiO<sub>2</sub> consist of dispersed domains 20-200 nm in diameter rather than continuous, flat monolayers. At an MPTMS concentration of  $5 \times 10^{-3}$  M, the domains are flat and composed of well-ordered monolayers with thiol headgroups uniformly distributed on the uppermost surface (Fig. 7a). As the MPTMS concentration increases, the domains are rougher and composed of less well-ordered monolayers and more disordered polymers with randomly distributed thiol headgroups on the uppermost surface (Fig. 7b). At an MPTMS concentration of  $4 \times 10^{-2}$  M, however, the domains are steep and composed of disordered polymers (Fig. 7c). This indicates that MPTMS molecules show good self-assembly at the MPTMS concentration of  $5 \times 10^{-3}$  M, but not above this concentration.

The effect of MPTMS concentration on the structure and morphology of MPTMS layers on  $\text{SiO}_2$  can be explained by the reaction mechanism of alkyltrimethoxysilanes with surface silanols, which is shown in Fig. 8. Alkylsiloxane hydrolysis either in solvents or on  $\text{SiO}_2$  surfaces, which is followed by subsequent dehydration on  $\text{SiO}_2$  surfaces, is the mechanism of SAMs formation [4, 8]. Hydrolysis in solvents favors self-polymerization, whereas hydrolysis on  $\text{SiO}_2$  surfaces causes the formation of SAMs. Thus, trace quantities of water in solvents or on  $\text{SiO}_2$  surfaces dominate the self-polymerization and dehydration reactions with surface silanols. Insufficient water either in solvents or on  $\text{SiO}_2$  surfaces impedes the hydrolysis reaction, and decelerates the subsequent surface dehydration reaction. On the contrary, excess water in solvents accelerates self-polymerization over the surface dehydration reaction.

McGovern et al. suggested that a water concentration of 1.5 ppm in solvents is optimum for forming closely packed OTS monolayers [4]. In our experiments, however, the water concentration in benzene was less than 30 ppm, and therefore probably higher than the suggested optimum concentration. The hydrolysis reaction in the solvent might occur more easily than on the  $\text{SiO}_2$  surface. Therefore, our experimental results can be explained by the following mechanism. At low MPTMS concentrations (Fig. 8a), hydrolyzed MPTMS molecules diffuse to the  $\text{SiO}_2$  surface to form smooth, well-ordered SAMs, rather than polymerize with each other in the solution. At high MPTMS concentrations (Fig. 8b), before they can diffuse to the  $\text{SiO}_2$  surface, more MPTMS molecules are hydrolyzed by water in the solution and polymerize there, rather than forming SAMs on the  $\text{SiO}_2$  surface. The sub-micrometer-sized polymer particles diffuse to and react with the  $\text{SiO}_2$  surface, which leads to the formation of rough polymer layers.

The domain formation for self-assembled OTS and APTES layers on  $\text{SiO}_2$  has also been clarified [7, 8]. Styrkas et al. found that self-assembled OTS on  $\text{SiO}_2$  forms rough layers composed of isolated domains and pinholes [7]. Vandenberg et al. found there are irregularities 200 nm in diameter and 20 nm high on  $\text{SiO}_2$  modified with APTES [8]. We believe that all of these results are related to alkylsiloxane concentrations and to trace quantities of water in solvents and on substrate

surfaces.

These results show that to prepare closely packed, well-ordered MPTMS monolayers on SiO<sub>2</sub>, both low MPTMS concentration and optimum water quantity are required. This principle is also applicable to the formation of other SAMs formed by alkyltrichlorosilane and alkyltrimethoxysilane derivatives with or without terminal functional groups.

#### 4. Conclusions

Self-assembled 3-mercaptopropyltrimethoxysilane (MPTMS, (CH<sub>3</sub>O)<sub>3</sub>SiCH<sub>2</sub>CH<sub>2</sub>CH<sub>2</sub>SH) layers on hydroxylated SiO<sub>2</sub> surfaces were prepared at MPTMS concentrations ranging from 5×10<sup>-3</sup> M to 4×10<sup>-2</sup> M. The surface structure and morphology of MPTMS layers were characterized by using XPS, contact angle measurements, SEM, and AFM. Both the structure and the morphology of MPTMS layers on SiO<sub>2</sub> surfaces depend on the MPTMS concentration. As MPTMS concentrations varied from 5×10<sup>-3</sup> M to 4×10<sup>-2</sup> M, MPTMS layers on SiO<sub>2</sub> surfaces consisted of dispersed domains 20-200 nm in diameter rather than continuous, flat monolayers. At an MPTMS concentration of 5×10<sup>-3</sup> M, the domains were flat and composed of well-ordered monolayers with thiol headgroups uniformly distributed on the uppermost surface. At an MPTMS concentration of 4×10<sup>-2</sup> M, however, the domains were steep and composed of disordered polymers with randomly distributed thiol headgroups on the uppermost surface. This indicates that MPTMS molecules show good self-assembly at the MPTMS concentration of 5×10<sup>-3</sup> M, but not above this concentration.

The effect of MPTMS concentration on the structure and morphology of MPTMS layers on SiO<sub>2</sub> is due to two competitive reactions, which depend on the trace quantity of water in the solvent and on the SiO<sub>2</sub> surface. One is the self-polymerization reaction of hydrolyzed MPTMS molecules, which forms sub-micrometer-sized particles condensing onto the SiO<sub>2</sub> surface. The other is the dehydration reaction of hydrolyzed MPTMS molecules with surface silanols, which forms well-ordered MPTMS monolayers on the SiO<sub>2</sub> surface. Our research suggests that both the MPTMS

and water concentrations are controlling factors for the preparation of SAMs, and must be precisely controlled to obtain well-ordered, self-assembled MPTMS layers.

## Acknowledgements

This work was supported by the "Research for the Future" Program of the Japan Society for the Promotion of Science (JSPS-RFTF 96P00402). We thank Prof. Shinichi Nakao and Mr. Shinya Maenosono for assisting with the contact angle and AFM measurements, and we thank Mr. Toshio Ohsawa, Ms. Yoshiko Tsuji, and Dr. Seiichi Takami (Department of Biochemistry and Engineering, Tohoku University) for helpful discussions and comments.

## References

- [1] A. Ulman, *An Introduction to Ultrathin Organic Film, from Langmuir-Blodgett to Self-Assembly*, Academic Press, New York, 1991.
- [2] P. Silberzan, L. Leger, D. Ausserre, J. Benattar, *Langmuir* 7 (1991) 1647.
- [3] J. D. Le Grange, J. L. Markham, *Langmuir* 9 (1993) 1749.
- [4] M. E. McGovern, K. M. R. Kallury, M. Thompson, *Langmuir* 10 (1994) 3607.
- [5] S. R. Cohen, R. Naaman, J. Sagiv, *J. Chem. Phys.* 90 (1986) 3054.
- [6] T. Nakagawa, K. Ogawa, *Langmuir* 10 (1994) 367.
- [7] D. A. Styckas, J. L. Keddie, J. R. Lu, T. J. Su, *J. Appl. Phys.* 85 (1999) 868.
- [8] E. T. Vandenberg, L. Bertilsson, B. Liedberg, K. Uvdal, R. Erlandsson, H. Elwing, I. Lundstrom, *J. Colloid Interface Sci.* 17 (1991) 103.
- [9] K. M. R. Kallury, P. M. Macdonald, M. Thompson, *Langmuir* 10 (1994) 492.
- [10] K. C. Vrancken, K. Possemiers, P. Van Der Voort, E. F. Vansant, *Colloid and Surf. A* 98 (1995) 235.

- [11] T. J. Horr, P. S. Arora, *Colloid and Surf. A* 126 (1997) 113.
- [12] B. Porsch, J. Kratka, *J. Chromatogr.* 543 (1991) 1.
- [13] K. M. R. Kallury, Lee, W. E. Lee, M. Thompson, *Anal. Chem.* 65 (1993) 2459.
- [14] N. P. Hughes, D. Heard, C. C. Perry, R. J. P. Williams, *J. Phys. D* 24 (1991) 146.
- [15] J. Hong, H. Yang, M. Jo, H. Park, S. Choi, *Thin Solid Film* 308-309 (1997) 495.
- [16] Z. Xiao, J. Gu, D. Huang, Z. Lu, Y. Wei, *Appl. Surf. Sci.* 125 (1998) 85.
- [17] M. M. Walczak, C. Chung, S. M. Stole, C. A. Widrig, M. D. Porter, *J. Am. Chem. Soc.* 113 (1991) 2370.
- [18] P. E. Laibinis, G. M. Whitesides, D. L. Allara, Y. Tao, A. N. Parikh, R. G. Nuzzo, *J. Am. Chem. Soc.* 113 (1991) 7152.
- [19] P. E. Laibinis, G. M. Whitesides, *J. Am. Chem. Soc.* 114 (1992) 9022.
- [20] M. Volmer-Uebing, M. Stratmann, *Appl. Surf. Sci.* 55 (1992) 19.
- [21] C. W. Sheen, J. X. Shi, J. Martensson, A. N. Parikh, D. L. Allara, *J. Am. Chem. Soc.* 114 (1992) 1514.
- [22] Y. Gu, B. Lin, V. S. Smentkowski, D. H. Waldeck, *Langmuir* 11 (1995) 1849.
- [23] Q. Zhang, H. Huang, H. He, H. Chen, H. Shao, Z. Liu, *Surf. Sci.* 440 (1999) 142.
- [24] M. Fang, C. H. Kim, B. R. Martin, T. E. Mallouk, *J. Nanoparticle Research* 1 (1999) 43.
- [25] K. M. Kulinowski, P. Jiang, H. Vaswani, V. L. Colvin, *Adv. Mater.* 12 (2000) 833.
- [26] X. Huang, H. Huang, N. Wu, R. Hu, T. Zhu, Z. Liu, *Surf. Sci.* 459 (2000) 183.
- [27] L. T. Zhuravlev, *Langmuir* 3 (1987) 316.
- [28] J. M. Madeley, C. R. Richmond, *Z. Anorg. Allg. Chem.* 389 (1972) 82.
- [29] P. Laoharajanaphand, T. L. Lin, J. O. Stoffer, *J. Appl. Polym. Sci.* 40 (1990) 369.
- [30] A. Heise, H. Menzel, *Langmuir* 13 (1997) 723.

## Figure Captions

Fig. 1. XPS spectra of C(1s) for (a) bare SiO<sub>2</sub> substrate and SiO<sub>2</sub> substrates treated with (b)  $5.0 \times 10^{-3}$  M and (c)  $4.0 \times 10^{-2}$  M MPTMS.

Fig. 2. XPS spectra of S(2p) vs. take-off angle for SiO<sub>2</sub> substrates treated with (a)  $5.0 \times 10^{-3}$  M and (b)  $4 \times 10^{-2}$  M MPTMS.

Fig. 3. S/C atomic ratio measured with ARXPS for SiO<sub>2</sub> substrates treated with (a)  $5 \times 10^{-3}$  M and (b)  $4 \times 10^{-2}$  M MPTMS at take-off angles of 10°, 50°, and 90°.

Fig. 4. Water contact angle on SiO<sub>2</sub> substrates treated with MPTMS at MPTMS concentrations ranging from 0 to  $8.0 \times 10^{-2}$  M.

Fig. 5. Surface SEM images of (a) bare SiO<sub>2</sub> substrate and SiO<sub>2</sub> substrates treated with (b)  $5 \times 10^{-3}$  M, (c)  $2 \times 10^{-2}$  M, and (d)  $4 \times 10^{-2}$  M MPTMS.

Fig. 6. Surface AFM images of (a) bare SiO<sub>2</sub> substrate and SiO<sub>2</sub> substrates treated with (b)  $5 \times 10^{-3}$  M, (c)  $2 \times 10^{-2}$  M, and (d)  $4 \times 10^{-2}$  M MPTMS. The lower panels show cross-sectional contours along the diagonal from the top left to the bottom right of each AFM image shown above. Note that the scale of the vertical axis in all of the lower panels ranges from - 5 to + 5 nm, except for that in panel d, which ranges from - 20 to + 20 nm.

Fig. 7. Schematic diagram of the structure and morphology of MPTMS layers formed on SiO<sub>2</sub> at MPTMS concentrations of (a)  $5 \times 10^{-3}$  M, (b)  $2 \times 10^{-2}$  M, and (c)  $4 \times 10^{-2}$  M.

Fig. 8. Competitive reactions in the formation of self-assembled MPTMS layers on the SiO<sub>2</sub> surface: (a) surface dehydration on the SiO<sub>2</sub> surface; (b) self-polymerization in the solvent.

Table 1. Relative elemental compositions of SiO<sub>2</sub> surfaces after the treatment with MPTMS at MPTMS concentrations ranging from 5.0×10<sup>-3</sup> M to 4.0×10<sup>-2</sup> M, determined from XPS analysis.

MPTMS Concentration (M)	Si (%)	S (%)	O (%)	C (%)
0	27.4	0	68.7	3.9
5.0×10 <sup>-3</sup>	25.7	0.6	62.0	11.7
1.0×10 <sup>-2</sup>	24.4	1.4	59.7	14.5
2.0×10 <sup>-2</sup>	22.4	2.9	52.8	21.9
4.0×10 <sup>-2</sup>	18.7	5.2	43.3	32.8

Fig. 1

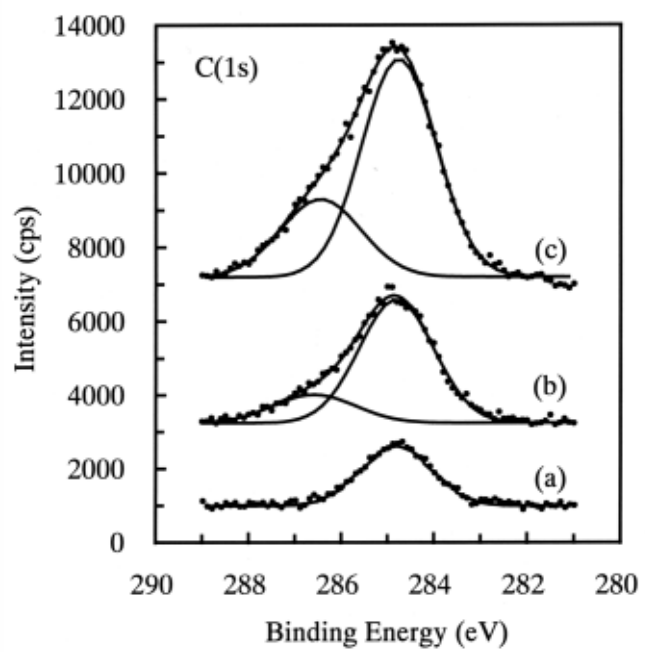


Fig. 2

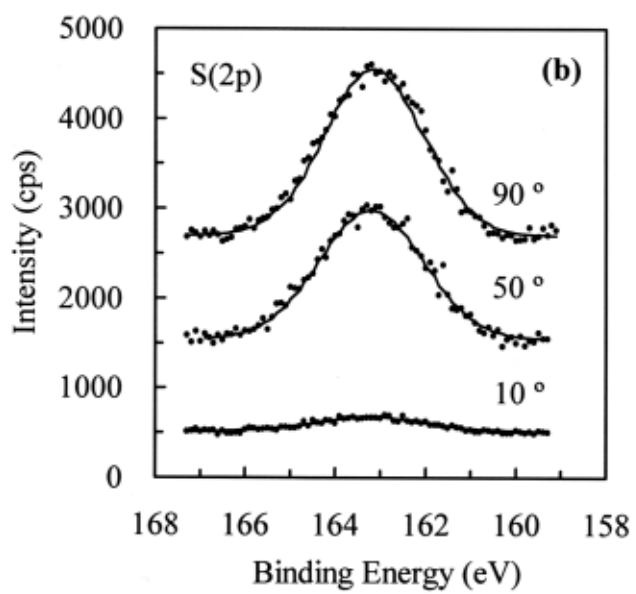
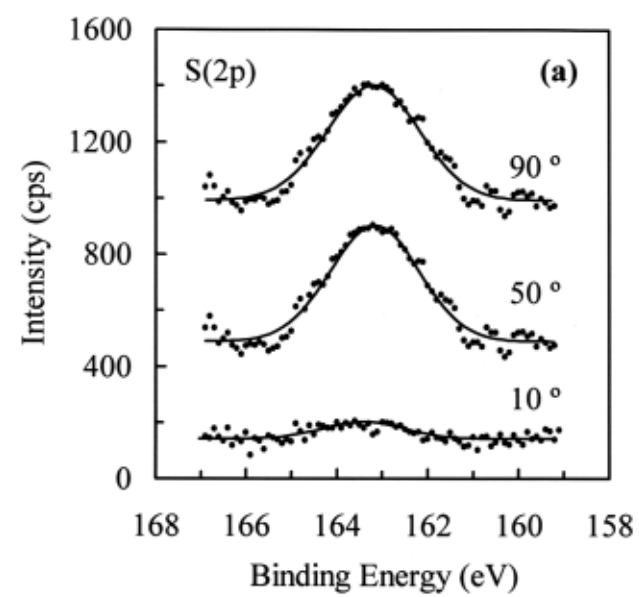


Fig. 3

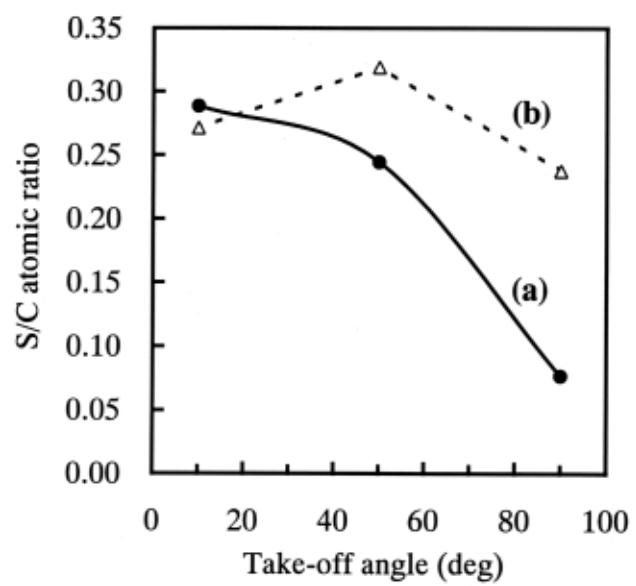


Fig. 4

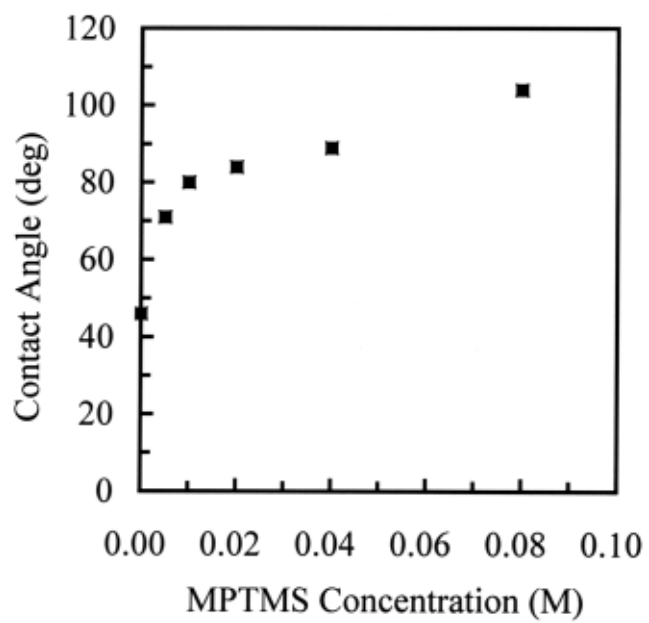


Fig. 5

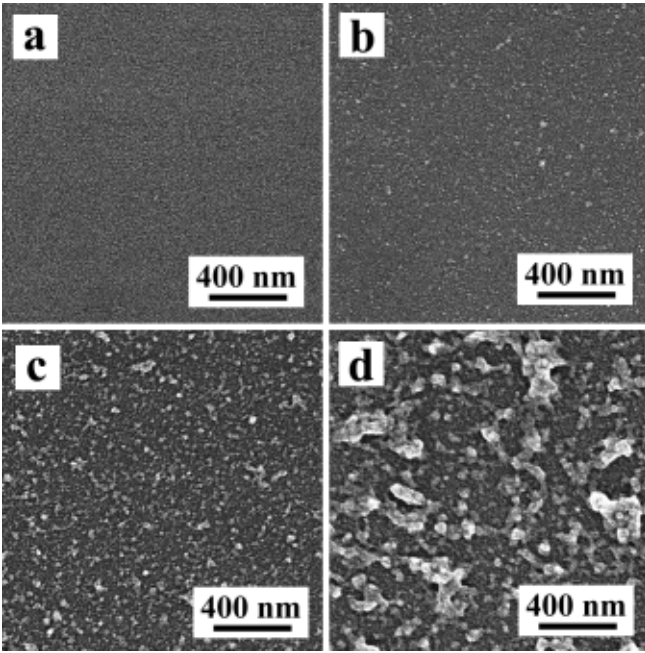


Fig. 6

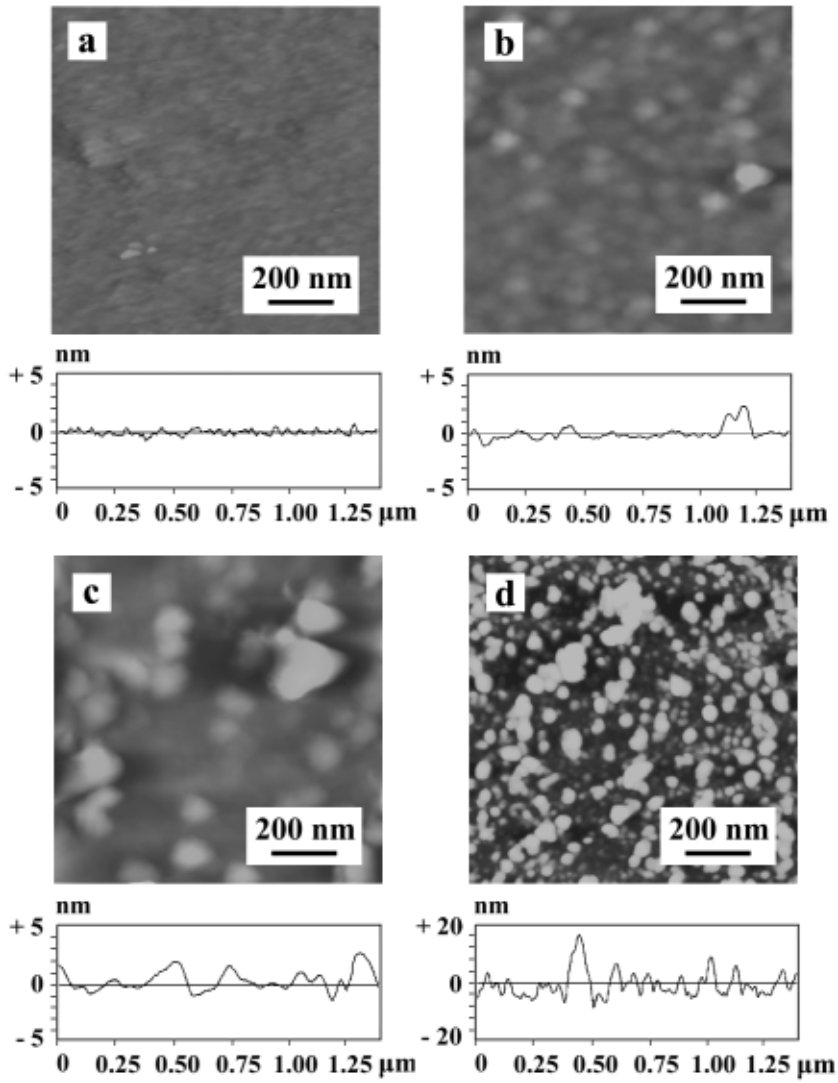


Fig. 7

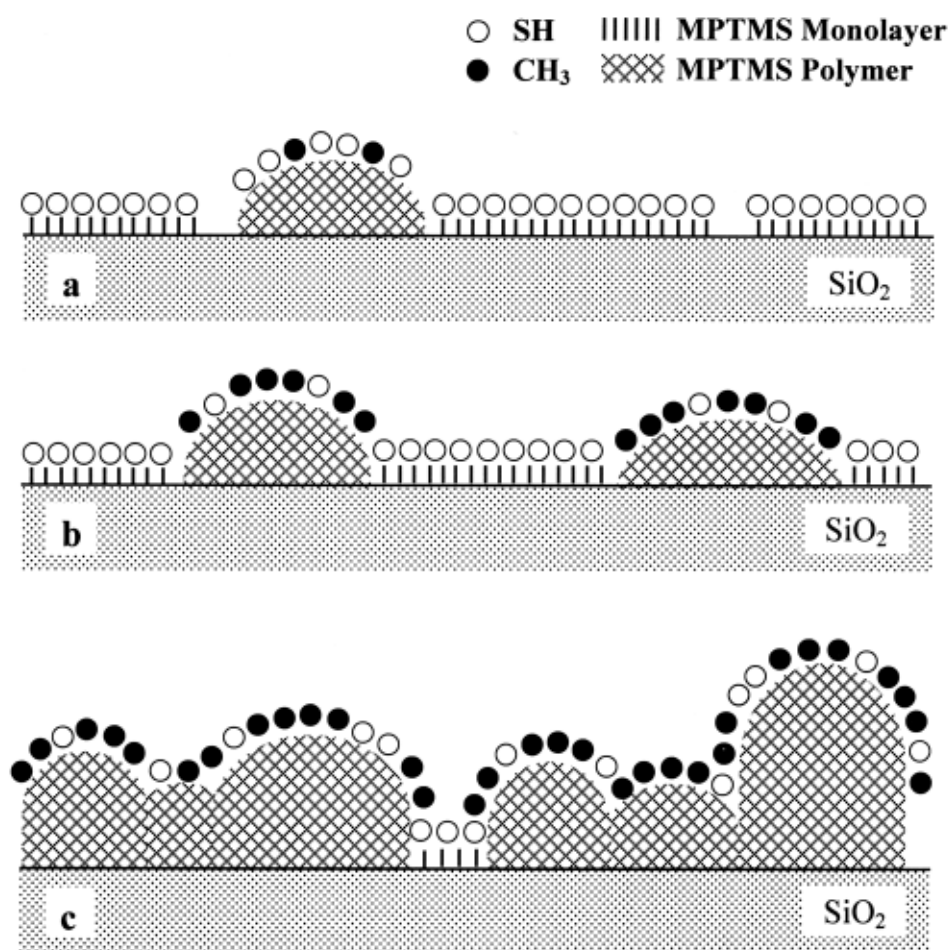


Fig. 8

